American Mineralogist, Volume 73, pages 470–486, 1988

Systems Fe-O and Cu-O: Thermodynamic data for the equilibria Fe-"FeO," Fe-Fe_3O_4, "FeO"-Fe_3O_4, Fe_3O_4-Fe_2O_3, Cu-Cu_2O, and Cu_2O-CuO from emf measurements

HUGH ST. C. O'NEILL[1]
Research School of Earth Sciences, Australian National University, Canberra, A.C.T. 2601, Australia

ABSTRACT

The chemical potential of oxygen (μ_{O_2}) defined by the reactions

$$1.5Fe + O_2 \rightleftharpoons 0.5Fe_3O_4,$$

$$2Fe + O_2 \rightleftharpoons 2\text{"FeO,"}$$

$$6\text{"FeO"} + O_2 \rightleftharpoons 2Fe_3O_4,$$

$$4Fe_3O_4 + O_2 \rightleftharpoons 6Fe_2O_3,$$

$$4Cu + O_2 \rightleftharpoons 2Cu_2O,$$

and

$$2Cu_2O + O_2 \rightleftharpoons 4CuO$$

has been determined using an electrochemical method with calcia-stabilized zirconia solid electrolytes. The Fe + Fe_3O_4, Fe + "FeO," and Cu + Cu_2O equilibria were measured using air as the reference, and these results are thus absolute determinations of μ_{O_2}. Cu + Cu_2O and Fe + "FeO" were then used as reference electrodes for other measurements reported both here and elsewhere.

The results for the μ_{O_2} values are [in $J \cdot mol^{-1}$, T in kelvins, with a reference pressure for O_2 of 1 bar (10^5 Pa)]

for Cu + Cu_2O (±62),

$$-347\,705 + 246.096T - 12.9053T \ln T \quad (750 < T < 1330),$$

for Fe + "FeO" (±100),

$$-605\,812 + 1366.718T - 182.7955T \ln T + 0.10359T^2 \quad (833 < T < 1042),$$
$$-519\,357 + 59.427T + 8.9276T \ln T \quad (1042 < T < 1184),$$
$$-551\,159 + 269.404T - 16.9484T \ln T \quad (1184 < T < 1450),$$

for "FeO" + Fe_3O_4 (±306),

$$-581\,927 - 65.618T + 38.7410T \ln T \quad (833 < T < 1270),$$

for Fe + Fe_3O_4 (±107),

$$-607\,673 + 1060.994T - 132.3909T \ln T + 0.06657T^2 \quad (750 < T < 833),$$

and for Cu_2O + CuO (±117),

$$-292\,245 + 377.012T - 23.1976T \ln T \quad (800 < T < 1300).$$

The standard enthalpy of formation of Fe_3O_4 is -1115.4 ± 0.2 $kJ \cdot mol^{-1}$, in excellent agreement with that deduced from the quartz-fayalite-iron and quartz-fayalite-magnetite equilibria at higher temperatures.

The results for the Fe_3O_4 + Fe_2O_3 equilibrium are less certain and have therefore not been presented in the form of a simple equation. For the other equilibria, the results represent a significant improvement in accuracy over existing measurements.

[1] Present address: Bayerisches Geoinstitut, Universität Bayreuth, Postfach 101251, 8580 Bayreuth, West Germany.

0003–004X/88/0506–0470$02.00

Introduction

The system Fe-O has been of interest for at least the past three millennia, although it is only in the past one hundred years or so that a thermochemical description has become available. Both the accuracy and internal consistency of the published thermodynamic data have increased over the years, so that there is now a firm consensus on most of the preferred values. Spencer and Kubaschewski (1978) provided a thorough and critical review of the published work, covering both phase-equilibrium studies and calorimetric data up to and including 1975. They gave selected values for most of the thermodynamic quantities and presented a phase diagram. To illustrate the amount of work that has gone into this system, it may be noted that Spencer and Kubaschewski (1978) listed no less than 35 experimental determinations of the oxygen fugacity defined by the Fe-"FeO" (iron-wüstite) equilibrium, covering the years 1927 to 1975, and employing a number of different experimental techniques.

There would therefore seem to be little point in further investigation of this system, unless a significant improvement in accuracy could be achieved. The present study was motivated in the belief that this might well be possible for the univariant equilibria in the system, by using an electrochemical method with oxygen-specific calcia-stabilized zirconia (CSZ) solid electrolytes.

The four isobarically univariant equilibria in the Fe-O system at 1 atm and subsolidus temperatures are

iron-magnetite,

$$1.5Fe + O_2 \rightleftharpoons 0.5Fe_3O_4, \quad (1)$$

iron-wüstite,

$$2Fe + O_2 \rightleftharpoons 2\text{"FeO,"} \quad (2)$$

wüstite-magnetite,

$$6\text{"FeO"} + O_2 \rightleftharpoons 2Fe_3O_4, \quad (3)$$

and magnetite-hematite,

$$4Fe_3O_4 + O_2 \rightleftharpoons 6Fe_2O_3. \quad (4)$$

The first three intersect at an isobaric invariant point at 1 atm near 833 K (Spencer and Kubaschewski, 1978), and "FeO" is only stable above this temperature. "FeO," wüstite, is written in quotation marks, because it always shows large deviations from the ideal FeO stoichiometry at atmospheric pressure. Considerable nonstoichiometry is also shown by Fe_3O_4 in equilibrium with Fe_2O_3 at high temperatures.

Previous thermodynamic studies from this laboratory (e.g., Holmes at al., 1986; O'Neill, 1987a, 1987b) have shown that it is generally possible to achieve a precision of the order of ± 100 J·mol^{-1} in the determination of the chemical potential of oxygen (μ_{O_2}) defined by univariant equilibria, by using an electrochemical method with simple metal + metal oxide mixtures as the reference electrode. This level of precision means that the uncertainty in the current values for the μ_{O_2} of the metal plus metal oxide reference would provide overwhelmingly the largest contribution to the total absolute accuracy of such experiments. Therefore, in order to get the most out of the method, it is necessary to calibrate at least one metal + metal oxide equilibrium against air, the absolute μ_{O_2} of which is, of course, known almost exactly. In fact, two such equilibria, Fe + "FeO" and also Cu + Cu_2O (copper-cuprite), were chosen for this primary calibration purpose, so that the results might be checked by measuring one against the other. The other equilibria in the Fe-O system were then measured using the above equilibria and also Ni + NiO (previously measured against both Fe + "FeO" and Cu + Cu_2O) as the reference oxygen buffers. For the sake of completeness, the Cu_2O + CuO (cuprite-tenorite) equilibrium was also determined.

The experimental method with the solid metal plus metal oxide buffers as reference electrodes has been fully described elsewhere (O'Neill, 1987a). However, the method using air as the reference is somewhat different; this method presents a number of additional experimental problems and will therefore be described below. Although the precision of the measurements reported in this paper can speak for themselves, that their accuracy is as good as is claimed can only be judged if a thorough appraisal of a number of experimental points is presented in some detail.

Experimental details

Design of electrochemical cells with air reference electrodes

High-temperature electrochemical cells using calcia-stabilized zirconia (CSZ) as an oxygen-specific electrolyte, and with air, or another gas, as the reference electrode, have often been used for thermodynamic measurements, e.g., Charette and Flengas (1968). Some more recent studies that give details of experimental designs, which may be compared to the design used in the present work, include Berglund (1976), Kemori et al. (1979), Jacobsson and Rosén (1981), Schwab and Küstner (1981), Comert and Pratt (1982), and Bannister (1984). Previous measurements from this laboratory on a number of metal + metal oxide oxygen buffers using air as the reference electrode have been reported by Holmes et al. (1986). The experimental design adopted in this study evolved out of the latter work, but it also incorporates a number of improvements aimed at increasing the already impressive accuracy achieved by Holmes et al. (1986). Therefore, in the description that follows, particular attention will be paid to these innovations; for a more complete description of some details, the reader is referred to Holmes et al. (1986) and O'Neill (1987a).

The experimental design is shown schematically in Figure 1. It consists essentially of two identical CSZ tubes of dimensions 8-mm outside diameter × 5-mm inside diameter × 300-mm length, 11 mol% CaO, which were supplied by the Nippon Chemical Ceramic Co. The upper CSZ tube contains the sample, and the arrangement of this half of the cell is exactly as previously described in O'Neill (1987a) for the analogous half of the cells with M + MO reference electrodes. The top of this CSZ tube is sealed with epoxy into a brass head attached to a shut-off valve followed by a three-way valve, which allows for thorough

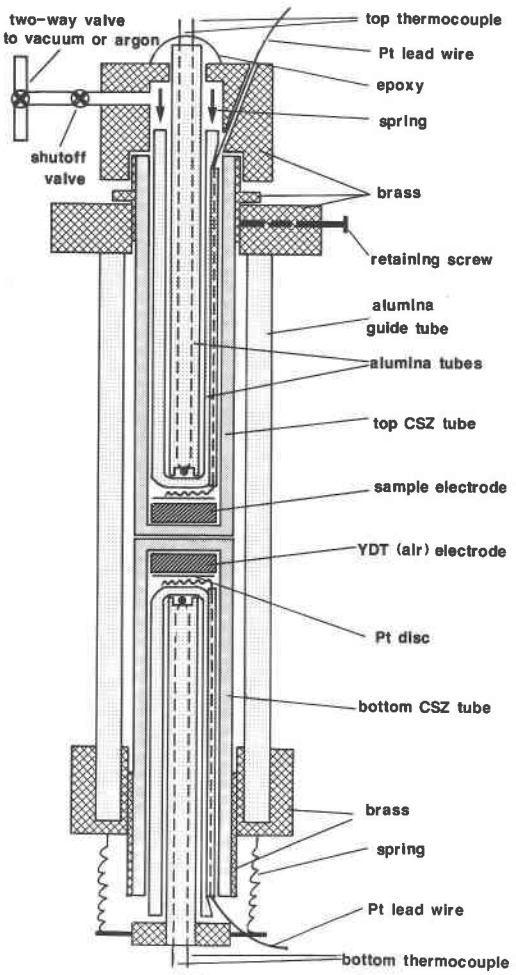

Fig. 1. Schematic diagram of the electrochemical cells with air as the reference electrode. The vertical scale is greatly compressed relative to the horizontal.

evacuation of the sample tube followed by filling with highly purified Ar gas. The sample is thus kept under a static atmosphere of Ar. The bottom CSZ tube contains the air electrode. The two tubes are inserted into a thick-walled (3-mm) alumina guide tube, which is carefully positioned along the vertical axis of a tube furnace (Deltech model DT-31-VT), the same one as used by Holmes et al. (1986). The bottom CSZ tube is supported on a pair of tension springs, which, since the tube is free to slide within the alumina guide tube, ensures that it is pressed firmly against the upper CSZ tube. The top tube is itself fixed in position with a screw. Two thermocouples are used, one sitting directly over the sample electrode, the other directly underneath the air reference electrode. The use of two thermocouples ensures that the entire working part of the cell is exactly positioned within the constant-temperature zone (or "hot spot") of the furnace. The distance between the two thermocouple beads is 8 mm, whereas the width of the constant-temperature zone [measured by Holmes et al. (1986) and taken to be that region of the furnace along the vertical axis within 0.5 K of the peak temperature] is only about 10 mm long. With the present system, however, the constant-temperature zone may be somewhat longer, since (1) the symmetrical arrangement of the two CSZ tubes ensures similar conductive heat losses both upward and downward and (2) the large thermal mass of the alumina guide tube should serve to smooth out the temperature gradient, as well as dampening any short-term fluctuations in temperature.

Holmes et al. (1986) observed that the position of the zone of constant temperature moves upward in the furnace with increasing temperature. The present arrangement allows the position of the cell to be adjusted during the course of an experiment, simply by loosening the screw holding the top CSZ tube and sliding both tubes either upward or downward, as required, within the alumina guide tube. Any temperature gradient across the cell would produce a thermoelectric emf, the magnitude of which depends on a number of factors—see Choudhary et al. (1980) for a detailed discussion and also an interesting paper by Alcock et al. (1977), who attempted to use this effect as an "entropy meter." From these references, a thermoelectric coefficient of about 0.5 $mV \cdot K^{-1}$ would be expected for the types of cell studied here; therefore, errors that are larger that the internal precision of the measurements would be introduced by a temperature gradient of only 1 K across the cell.

In most previous investigations using high-temperature electrochemical cells with air (or other gases), the gas electrode has consisted of Pt, often applied as a colloidal suspension of "platinum black." Pt foil or wire pressed firmly against the electrolyte also works effectively at high temperatures, and other noble metals or their alloys have sometimes been used. The purpose of the Pt, in addition to providing the electrical connection to the cell, is to catalyze the half-cell reaction:

$$O_2 \text{ (gas)} + 4e^- \text{ (electrode)} = 2O^{2-} \text{ (electrolyte)}.$$

However, below about 900 K, this process becomes increasingly inefficient, particularly if the surface area of the Pt coating has been reduced by long sintering at high temperature. This results in high electrode impedance and non-Nernstian behavior (Badwal, 1983) and sluggish response times. During the present work, it was indeed found that, with such electrodes at $T < 900$ K, anomalous, unstable, and irreproducible emf's (typically <2 mV) appeared in symmetric cells of the type air versus air, the emf's from which should, of course, always be zero in the absence of a temperature gradient across the cell.

Such phenomena have led the Australian CSIRO Division of Materials Science to investigate the use of urania-scandia solid solutions with the fluorite structure as gas electrodes (Badwal, 1983, 1984). An electrode of this type was successfully used by Bannister (1984) in his investigation of the Pb-PbO equilibrium against air at temperatures as low as 645 K. In the present study, this concept was adopted with the modification that, instead of a coating of urania-scandia, pellets of yttria-doped thoria (YDT) were used. YDT has been extensively employed as an oxygen-specific electrolyte, especially at low oxygen fugacities, as it retains virtually 100% oxygen ion conductivity to much lower f_{O_2} values than the stabilized zirconias [e.g., Choudhary et al. (1980)]. However, at higher oxygen fugacities, such as that of air, YDT becomes a p-type semiconductor, with electron holes and interstitial oxygen ions. A very noticeable property of YDT is that is appears white after sintering in a reduced atmosphere, but turns dark brown on heating in air, owing to the absorption of this excess oxygen. The change is perfectly reversible and occurs reasonably rapidly even at fairly low temperatures (e.g., ~750 K). The YDT pellets thus provide a small reservoir of oxygen in a suitable state at the air electrode. With air electrodes of this type, it proved possible to achieve emf's stable to ±0.1 mV in the air versus air cells down to 750 K.

The procedure for measuring the emf's of the electrochemical cells and of the thermocouples are given in O'Neill (1987a). The thermocouples were of the Pt-$Pt_{90}Rh_{10}$ type, and all the thermocouples used in this part of the study (i.e., with the air electrodes) were made from the same two spools of wire supplied by Johnson Matthey. All were calibrated against the melting point of Au (1337.58 K, IPTS 68), using small sections (~3 mm) of 0.5-mm-diameter Au wire, 99.99+% purity, supplied by Goodfellow Metals with an analysis that showed 7 ppm Co, 1 ppm Ag, and 1 ppm Cu as the only impurities. The Au wire was crimped over the thermocouple bead, and the thermocouple was placed in a dummy cell made by withdrawing the top CSZ tube shown in Figure 1 and replacing it with a CSZ tube plus alumina sheath tube, both with truncated ends. The thermocouples are thus calibrated in almost the exact configuration in which they are used. The calibrations were carried out by slowly heating the thermocouple through the melting temperature of Au while recording its emf on a chart-recorder and observing the plateau in the resulting trace. This plateau is generally sharp to ±0.001 mV, provided that the Au wire is fixed directly over the thermocouple bead and that neither the bead nor the wire come into contact with any ceramic part of the apparatus. After each calibration, the wires were pulled through the thermocouple tubing, the old bead plus Au cut off, and a new bead formed. Eighteen such calibrations carried out during the course of these experiments on eight different thermocouples (i.e., made from different sections of wire) gave a range in emf's at the Au point from 10.272 to 10.277 mV, with a single outlier at 10.281 mV, and a mean of 10.275 ± 0.002 mV. Although this value is somewhat lower than that used by IPTS 68 as the fixed point (10.3343 mV, exactly) it is still well within the recommended range for Pt-$Pt_{90}Rh_{10}$ thermocouples of 10.300 ± 0.050 mV (Rossini, 1970). A fairly large number of similar calibrations on thermocouples made from wire from various different spools (all supplied by Johnson Matthey) have yielded results in the range 10.298 to 10.336 mV, and therefore it would seem that the low calibration emf is a characteristic of the particular batch of wire used during this study. The constant of proportionality calculated from the ratio of the ideal to the measured emf of the thermocouples at the Au point was then used to correct the thermocouple emf's at all other temperatures. The assumptions inherent in this procedure were checked for two thermocouples by measuring the melting point of NaCl, as described by O'Neill (1987a). Most of the experimental data reported in this study were obtained at temperatures lower than the melting point of Au and thus fall between this temperature and the ice point (actually the melting point of ice at ambient pressure), which is used as the reference temperature. This temperature calibration is felt to be accurate to ±0.3 K.

The entire experimental arrangement was tested by measuring the emf produced by the symmetrical cell

Pt, YDT (air)|CSZ|YDT (air), Pt.

For this cell, the sample pellet in the top CSZ tube (shown in Fig. 1) was replaced with a YDT pellet similar to the one in the bottom half of the cell and identical in size to the sample pellets. The top CSZ tube, plus alumina sheath and thermocouple tube, was also not sealed in the brass head, but left open to the atmosphere, so that the top half of the assembly became effectively identical to the bottom half. The symmetrical cell was then heated to a number of different temperatures in the range anticipated for the actual measurements of the oxygen buffers, i.e., 750–1400 K. It was found that the resistance of the cell becomes large relative to the resistance of the emf-measuring circuit below about 750 K, and therefore measurements were not attempted below this temperature.

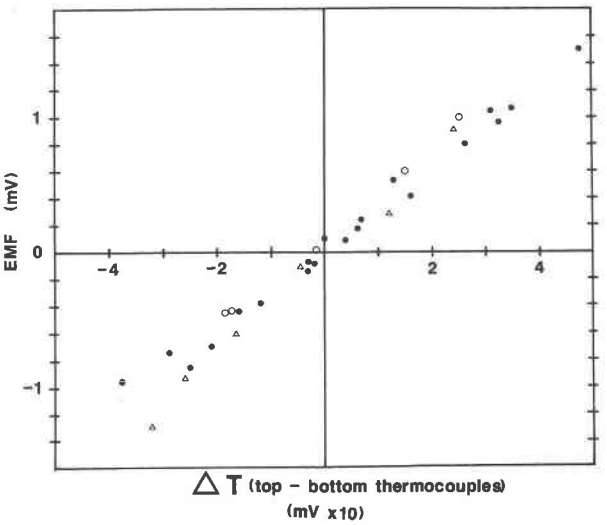

Fig. 2. The emf of the symmetrical cell Pt, air|CSZ|air, Pt as a function of the difference ΔT between the top and bottom thermocouples of the cell (shown in Fig. 1) at the following approximate temperatures: △, 1020 K; ●, 1150 K; ○, 1350 K.

At each temperature, the cell assembly was moved through a number of different positions up and down the region close to the constant-temperature zone, and the emf of the cell was recorded at these different positions together with the emf of both the top and the bottom thermocouples, thus measuring the effect of the temperature gradient across the cell. Representative results are shown in Figure 2, from which it will be seen that when the two thermocouples record the same temperature, the emf of the cell is, as it should be, effectively zero (± <0.1 mV). This also implies that any lateral temperature gradients are unimportant. A similar symmetric cell (air vs. air) test was conducted by Holmes et al. (1986). In contrast with the present results, they found small (<1.5 mV) excess emf's across the cell although the cell was thought to be positioned exactly in the constant-temperature zone of the furnace. However, the location of the constant-temperature zone was not determined in situ; therefore, despite all precautions, the positioning of the cell may not have been exactly right. Furthermore, these excess or residual emf's changed with temperature and also showed some scatter at lower temperatures (<1300 K), which might possibly reflect a problem with the efficiency of the Pt coating used for the air electrodes, as discussed above.

For the actual measurements reported in this study, the position of the cell was adjusted, if necessary, so that the observed difference between the two thermocouples was less than ±0.5 K. A correction to zero temperature gradient was then made from an empirical calibration of relative emf versus temperature gradient, obtained at a couple of different temperatures during the course of the experiment. This procedure avoids the tediousness of precisely adjusting the position of the cell for every measurement.

Chemical potential of oxygen in air

The oxygen content of dry air is remarkably constant worldwide at 20.946%. The chemical potential of oxygen in air is

therefore given by

$$\mu_{O_2}^{air} = RT \ln[0.20946(P_{total} - P_{H_2O})] \quad (5)$$

where P_{total} is the atmospheric pressure, and P_{H_2O} is the vapor pressure of water in the atmosphere. It is not unusual in most climates for P_{total} to vary by ± 15 mbar (1.5×10^3 Pa), according to the local weather conditions. Were this factor to be ignored, it would cause a change in $\mu_{O_2}^{air}$ of ± 150 J·mol^{-1} at, for example, 1200 K. This variation is greater than the potential precision of the method. Therefore, for each datum, P_{total} was measured with a Hg barometer. The readings were corrected for the absolute value of gravity as measured adjacent to the laboratory and are thought to be accurate to ± 2 mbar. As far as possible, taking data during rapid changes in atmospheric pressure conditions was avoided. P_{H_2O} was also measured, using a wet-and-dry-bulb psychrometer kindly loaned by the Canberra Bureau of Meteorology. Fortunately, Canberra enjoys a dry climate, and since most of this work was undertaken during the winter months, the absolute value of P_{H_2O} was fairly low. (During the course of these experiments it was observed to vary from 5 to 20 mbar, and was typically about 8 mbar.) Thus, although the accuracy of the psychrometer is not known, it would seem unlikely that the error in P_{H_2O} is greater than ± 2 mbar; therefore, the total error in $\mu_{O_2}^{air}$ will be less than ± 40 J·mol^{-1}, excluding the contribution from any errors in temperature measurement.

Precision, accuracy, and demonstration of equilibrium

In what follows, "precision" is taken to mean the measure of the scatter expected in the data, whereas "accuracy" refers to the absolute deviation of the measurements from the true value. Precision of course contributes to accuracy.

Temperatures were recorded to ± 0.1 K. Monitoring of the thermocouple emf over extended periods of time showed that short-term fluctuations, caused either by fluctuations in the actual temperature of the furnace (which are nearly completely damped in the cell by the large thermal mass of the alumina guide tube; see Fig. 1) or by fluctuations in the emf-measuring circuit, are also about 0.1 K or at about the resolution of the actual measurements. The temperature dependence of the cell emf and the dependence of the cell emf on thermal gradient are both approximately 150 J·K^{-1}·mol^{-1}, and therefore the precision expected from the combined uncertainties in measuring both thermocouples is about ± 50 J·mol^{-1}. The precision in the measurements of the air reference electrode is equal to the accuracy and is about ± 40 J·mol^{-1}. The emf of the cell was recorded to ± 0.05 mV and is precise to ± 0.1 mV, which is equivalent to ± 40 J·mol^{-1}. Therefore, the total precision of the measurements is ± 75 J·mol^{-1}, which corresponds to ± 0.003 log f_{O_2} at 1200 K. For an estimate of the total accuracy of the measurements, two other factors must be taken into consideration. First, there is the accuracy of the thermocouple calibration at the melting point of Au, and its extrapolation to other (mainly lower) temperatures. This has been estimated earlier to be ± 0.3 K, which, for the temperature dependence of the cell emf values in this study, contributes another ± 50 J·mol^{-1} to the absolute uncertainty.

The second factor affecting the total accuracy is potentially of far greater magnitude and concerns the attainment of equilibrium by the oxygen buffer. Particularly important is the possibility that oxygen may leak from the atmosphere into the electrode, either because of the finite physical permeability of the CSZ tube or because the finite electronic conductivity causes a short circuit from the air reference electrode. An oxygen leak will result in a decrease of the emf of the cell, and consequently the μ_{O_2} of the buffer will appear erroneously high. At higher temperatures, oxygen leaks always occur with the type of CSZ tube used in this study, not only in the experiments with air, but also in those with solid metal + metal oxide reference electrodes (see, for example, O'Neill, 1987a). Since the amount of oxygen in the Ar gas above the latter is minute, it is probably the nonzero electronic conductivity that is to blame, rather than the physical passage of gas through the tube. Finite electronic conductivity is still consistent with otherwise ideal behavior of the electrolyte, provided that such electronic conductivity remains a very small fraction of the total (ionic + electronic) conductivity—less than 1% is usually considered the limit. The temperature above which the decrease of the cell emf becomes evident varies from run to run, even with identical cells, but tends to be between 1200 and 1350 K. At lower temperatures, at least with simple metal + metal oxide electrodes, the cell emf remains constant to within ± 0.2 mV over periods of days.

The Cu + Cu_2O and Fe + "FeO" equilibria were in fact specifically chosen for the primary measurements against air, because empirical experience in this laboratory, backed up by the polarization experiments of Worrell and Iskoe (1973), suggests that these two mixtures are the most reactive of the common metal + metal oxide oxygen buffers and hence will be least subject to polarization. To minimize the problem at higher temperatures (>1300 K), measurements were obtained as quickly as possible (i.e., about 30–40 min after changing furnace temperature). If any untoward decrease in cell emf occurred, the temperature was either lowered or the run abandoned. The times typically allowed for equilibration at lower temperatures were, very approximately, 12 h at $T < 900$ K, 6 h at $900 < T < 1050$ K, and 3 h at $1050 < T < 1300$ K. In all cases, the emf was judged to be constant (± 0.05 mV) before the reading was taken. On increasing temperature, the emf values were usually observed to change to the new value almost instantly (i.e., as fast as the change in temperature registered by the thermocouples) at $T >$ 900 K, but took rather longer at lower temperatures. The time required to reach stable emf values on decreasing temperature was slightly longer.

Reversibility of the cells, and hence equilibrium, was demonstrated by (a) obtaining data after both increasing and decreasing temperature, (b) passing a small current through the cell, or (c) evacuating the electrode compartment and filling it with an oxidizing or reducing gas such as air or Ar-CH_4, before refilling with purified Ar. Options (b) and (c) were only used at higher temperatures (>1000 K), and only toward the end of a run.

Materials

Cu_2O and "FeO" were prepared from Cu and CuO and from Fe and Fe_2O_3, respectively, mixed in the appropriate proportions but with a slight excess of metal and sintered at 1000 °C for ~8 h under a flowing stream of Ar, which was purified by passing successively over activated charcoal, phosphorus pentoxide, and Ti chips at 800 °C. Fe_2O_3 was sintered in air at 1000 °C for ~24 h; this treatment causes a change in color from brick red to deep maroon, and the XRD analysis of the sintered material gave a pattern corresponding to well-crystallized α-Fe_2O_3. Fe_3O_4 was used either as supplied by the manufacturers or after sintering in a flowing CO-CO_2 gas mixture corresponding to the quartz-fayalite-magnetite buffer; no difference was observed in the performance of the cells using either material. CuO, Cu, and Fe were used as supplied, without further treatment. All chemicals were stated by the manufacturers to be of >99.9% purity, with the exception of Fe metal, which was of >99.5% purity.

TABLE 1. Results from the cell Pt, Cu + Cu_2O|CSZ|$YDT_{(air)}$, Pt

T (K)	$-\mu_{O_2}$ (kJ·mol^{-1})	T (K)	$-\mu_{O_2}$ (kJ·mol^{-1})	T (K)	$-\mu_{O_2}$ (kJ·mol^{-1})
882.0	207.91	930.3	200.84	1221.0	159.20
846.7	213.03	945.7	198.59	1233.1	157.49
828.5	215.59	960.6	196.46	1245.2	155.82
809.6	218.37	975.4	194.31	1256.9	154.15
790.5	221.23	989.9	192.26	1268.2	152.57
770.5	224.26	1004.0	190.21	1279.2	151.02
749.6	227.35	1018.0	188.22	1290.6	149.47
760.2	225.84	1032.3	186.15	1301.1	147.95
770.7	224.19	1045.4	184.25	1312.0	146.40
780.8	222.61	1058.0	182.38	1322.6	144.93
790.9	221.13	1071.2	180.50	1257.4	154.07
800.6	219.70	1084.2	178.64	1234.6	157.29
810.4	218.26	1097.2	176.80	1163.1	167.39
819.6	216.90	1110.2	174.92	1322.8	144.88
828.9	215.58	1123.3	173.11	1332.2	143.55
838.1	214.23	1136.2	171.26	1301.4	147.88
847.2	212.93	1148.7	169.46	1279.7	150.95
856.2	211.64	1161.8	167.60	1211.9	160.45
865.0	210.33	1111.0	174.87	1187.6	163.92
873.3	209.14	1174.0	165.87	1084.8	178.57
890.6	206.61	1186.0	164.17	1058.5	182.32
898.5	205.43	1198.4	162.40	1031.0	186.24
914.6	203.19	1210.5	160.70	1002.2	190.39
906.9	204.25	1136.2	171.28		

Note: The order is that in which the measurements were made. The reference pressure is 1 bar (10^5 Pa).

The YDT pellets were made by precipitating solutions of thorium nitrate and yttrium nitrate (10 mol% Y_2O_3) with ammonia solution. The precipitate was dried in stages to 1000 °C, and the powder so obtained was pressed into pellets and sintered in air at 1550 °C for 3 d.

RESULTS

Cu + Cu_2O

The results of the measurements on the cell

$$\text{Pt, Cu + Cu}_2\text{O} \mid \text{CSZ} \mid \text{YDT}_{(\text{air})}, \text{Pt} \qquad \text{(I)}$$

are given in Table 1. All such data, both here and subsequently, have been corrected to a standard reference pressure of 1 bar (10^5 Pa). The range of temperature covered is from 750 K, the lowest possible with the present apparatus, to 1330 K, just below the Cu + Cu_2O melting eutectic.

The available calorimetric data for Cu and Cu_2O are of excellent quality and are also unusually accurate. A comprehensive assessment is presented in the JANAF tables (Chase et al., 1982), which is largely based on the work of Mah et al. (1967). A thorough discussion of the Cu-O system, including the phase diagram, has been given by Santander and Kubaschewski (1975), who showed that the solubility of oxygen in solid Cu is so small that it would have a totally negligible effect on the thermodynamic properties of Cu. Unfortunately, these authors reported that no data exist for the stoichiometric range of Cu_2O, and therefore it will be assumed that the thermodynamic data for this substance may be applied without correction to Cu_2O in equilibrium with Cu.

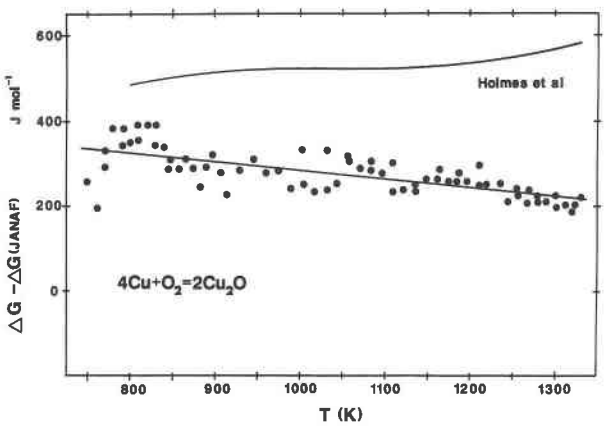

Fig. 3. Comparison of the results for the free energy of the reaction 4Cu + O_2 = $2Cu_2O$ with those derived from calorimetric data as assessed in the JANAF tables (Chase et al., 1982). Also shown is the curve for the earlier results from this laboratory by Holmes et al. (1986).

Values for the Gibbs free energy of the reaction

$$4\text{Cu} + \text{O}_2 = 2\text{Cu}_2\text{O} \qquad (6)$$

were taken from the values of $\Delta_f G^0_m$ tabulated at 100-K intervals for Cu_2O in the JANAF tables in the range 700 to 1300 K inclusive and, after, correction from the reference pressure of 1 atm to 1 bar, were fitted to an expression of the form $A + BT + CT \ln T$ to give, in J·mol^{-1},

$$\mu_{O_2,\text{JANAF}}^{(\text{Cu+Cu}_2\text{O})} = -348\,195 + 246.301T - 12.9053T \ln T. \qquad (7)$$

The standard deviation of this fit is 12 J·mol^{-1}, with a maximum deviation of 16 J·mol^{-1}; therefore, the three-term expression perfectly describes the calorimetric data in this temperature range. The deviations $\Delta\mu_{O_2} = \mu_{O_2,\text{obs}} - \mu_{O_2,\text{JANAF}}$ were calculated for each datum in Table 1, and the results have been plotted as a function of datum temperature in Figure 3. This procedure is equivalent to a third-law analysis of the experimental data.

The agreement between the present results and the calorimetric data is exceptionally good. Regression of $\Delta\mu_{O_2}$ vs. T gives (in J·mol^{-1})

$$\Delta\mu_{O_2}\ (\pm 38) = (490 \pm 26) - (0.205 \pm 0.025)T. \qquad (8)$$

Thus both the position and slope of the emf measurements are well within the very tight constraints imposed by the calorimetric data. The standard deviation of the measurements is only ±38 J·mol^{-1} (<0.002 log f_{O_2} at 1200 K). The absolute precision of the experimental method has been estimated previously to be ±75 J·mol^{-1}; therefore, if twice the standard deviation of the measurements is taken to be the observed precision, the agreement between the observed and theoretical precisions is exact. This implies that there is no error due to lack of equilibration of the Cu + Cu_2O assemblage.

There are a number of reasons why the results on Cu + Cu_2O might be especially good. First, the polarization

TABLE 2. Results from the cells Pt, Fe + "FeO" | CSZ | $YTD_{(air)}$, Pt

T (K)	$-\mu_{O_2}$ (kJ·mol^{-1})	T (K)	$-\mu_{O_2}$ (kJ·mol^{-1})	T (K)	$-\mu_{O_2}$ (kJ·mol^{-1})
		Run 1			
850.1	417.09	1046.8	392.13	1302.7	358.60
885.4	412.66	975.7	401.41	1313.9	357.12
918.7	408.85	1188.2	373.61	1324.3	355.75
949.8	404.51	1200.0	372.08	1334.3	354.40
979.9	400.70	1074.7	388.51	1153.7	377.90
1006.5	397.41	1100.4	385.10	1236.3	367.19
947.0	405.02	1211.4	370.57	1314.0	357.14
915.6	409.01	1223.8	368.92	1345.3	352.97
882.6	413.21	1235.4	367.40	1355.7	351.60
864.7	415.58	1126.5	381.62	1366.1	350.21
899.0	411.25	1246.5	365.93	1376.1	348.90
931.3	407.05	1257.9	364.46	1385.9	347.59
962.1	403.03	1269.7	362.93	1395.9	346.29
1163.9	376.83	1280.9	361.44	1405.7	345.00
1175.9	375.23	1292.0	359.97		
		Run 2			
882.8	413.12	1061.0	390.39	1187.9	373.56
899.8	410.88	1087.5	386.86	1211.7	370.55
915.9	408.85	1113.4	383.46	1236.4	367.07
947.3	404.87	1138.9	380.09	1259.6	364.16
977.8	400.94	1163.1	376.89	1060.7	390.39
1033.9	393.98				

TABLE 3. Results from the cells Pt, Fe + Fe_3O_4 | CSZ | $YTD_{(air)}$, Pt

T (K)	$-\mu_{O_2}$ (kJ·mol^{-1})	T (K)	$-\mu_{O_2}$ (kJ·mol^{-1})	T (K)	$-\mu_{O_2}$ (kJ·mol^{-1})
		Run 1			
811.4*	422.57	866.4	415.10	1151.9	378.52
820.9*	421.14	875.0	413.87	1176.1	375.41
830.6*	419.73	932.4	406.73	1201.6	371.77
837.6**	418.67	1021.1	395.51	1224.9	368.69
849.3**	416.96	1047.8	392.07	1247.6	365.73
857.8	416.17	1126.8	381.79		
		Run 2			
755.2*	431.15	868.0**	414.78	1034.1	393.88
764.2*	429.65	885.0**	412.59	1047.7	392.11
774.9*	428.06	901.7**	410.47	1060.9	390.40
784.2*	426.77	917.8	408.66	1074.0	388.72
793.5*	425.33	933.7	406.66	1086.4	387.16
803.1*	423.94	949.0	404.68	975.6	401.52
812.7*	422.53	964.2	402.74	1099.1	385.46
822.8*	420.94	979.0	400.87	1112.0	383.84
832.4*	419.49	992.5	399.25	1125.0	382.09
850.0**	417.13	1006.6	397.43	1137.7	380.44
859.0**	415.90	1020.7	395.62	1150.6	378.73
		Run 3			
750.7*	431.68	790.9*	425.57	819.6*	421.36
759.9*	430.40	800.4*	424.17	829.1*	419.95
770.9*	428.52	809.8*	422.67	846.5**	417.33
780.7*	427.11				

Note: Molar ratio of Fe to Fe_3O_4 is 4 to 1 for runs 1 and 2, and 1 to 2 for run 3.

* ($Fe + Fe_3O_4$) data; all others (Fe + "FeO"), except those marked with double asterisk.

** Status uncertain; possibility of reaction to "FeO" incomplete.

measurements of Worrell and Iskoe (1973) show that the Cu + Cu_2O electrode is approximately an order of magnitude more reactive than Fe + "FeO" at the same temperature and two orders of magnitude more reactive than Ni + NiO. The latter two are oxygen buffers that are themselves widely regarded as being highly reactive and easy to use; therefore Cu + Cu_2O might well be the most reactive of all the common metal + metal oxide electrodes. Second, the Cu + Cu_2O pellets are extremely soft and deform easily at high temperature to provide an essentially perfect electrode-electrolyte interface in the cell. Indeed they are impossible to extract from the CSZ tube after a run, unlike virtually all other mixtures I have studied. Third, no ternary phases are known to the Cu-Cu_2O-ZrO_2-CaO system; thus, there would seem to be little possibility of any side reactions in the cell. Certainly, no evidence of any such reaction was noted (the Cu + Cu_2O mixture may be cleaned out of the CSZ tubes very effectively with dilute acid, leaving an almost unmarked electrolyte surface). Fourth, the Cu + Cu_2O equilibrium buffers the oxygen fugacity at quite high values. The cell emf is only approximately half of that for the Fe + "FeO" buffer, and consequently any oxygen leakage due to electronic conduction should also be only half that for Fe + "FeO."

The slight difference between the emf measurements and the calorimetric data calculated from the regression analysis has been used to amend the expression for the chemical potential of oxygen defined by the Cu + Cu_2O equilibrium to (in J·mol^{-1})

$$\mu_{O_2}^{(Cu+Cu_2O)}\ (\pm 62) = -347\,705 + 246.096T - 12.9053T \ln T \qquad (9)$$

where the uncertainty in the parenthesis is ±1 standard deviation and includes the observed experimental precision in the results together with a contribution of ±50 J·mol^{-1} from the estimated possible error in the thermocouple calibration of ±0.3 K. This latter factor was omitted (by oversight) from earlier statements of these results in O'Neill (1987a, 1987b).

Also shown in Figure 3 is the curve reported in Holmes et al. (1986). The agreement with the present results is very good and is within the combined experimental uncertainties of the two studies. However, the present results are to be preferred, owing to the elimination of some of the potential errors in the experimental method reported in Holmes et al. (1986). A comprehensive comparison with other experimental work is presented in Holmes et al. (1986) and will therefore not be repeated here.

Fe + "FeO"

Results from cells of the type

$$\text{Pt, Fe + "FeO" | CSZ | } YDT_{(air)}\text{, Pt} \qquad \text{(II)}$$

are given in Table 2, and those from the cells

$$\text{Pt, Fe + } Fe_3O_4 \text{ | CSZ | } YDT_{(air)}\text{, Pt} \qquad \text{(III)}$$

are given in Table 3 for Fe + Fe_3O_4 mixtures in the molar ratio 4 to 1. Fe + Fe_3O_4 reacts rapidly to "FeO" at temperatures above the isobaric invariant point at which Fe, "FeO," and Fe_3O_4 coexist, and therefore most of the data from these cells appertain to the Fe + "FeO" equilibri-

um. Each low-temperature datum representing the Fe + Fe_3O_4 equilibrium is denoted by an asterisk and will be discussed later. A few additional points, although being in the Fe + "FeO" region, seem not to have fully equilibrated and were excluded from the following analysis. These data are marked by double asterisks. Two runs were done for each type of cell, and the temperature range covered is 840 to 1400 K.

Holmes et al. (1986) provided expressions for the chemical potential of oxygen defined by the Fe + "FeO" equilibrium as a function of temperature, based on the earlier electrochemical measurements in this laboratory. These expressions were also shown to be fully compatible with the best available calorimetric data for wüstite (JANAF, Stull and Prophet, 1971), although it may be noted that the application of such data is made somewhat uncertain owing to the large degree of nonstoichiometry shown by this phase. These expressions [there are three of them, corresponding to the temperature regions below the Curie point in Fe (1042 K), between the Curie point and the $\alpha \rightarrow \gamma$ transition (1184 K), and above the $\alpha \rightarrow \gamma$ transition] have been used to illustrate the present results, by plotting the difference, $\Delta\mu_{O_2}$ (Holmes et al., 1986), as a function of temperature in Figure 4. This procedure is similar to that already used for the Cu + Cu_2O equilibrium.

The agreement between the present results and the earlier ones is again very good. Regression analysis of the differences gives (in J·mol^{-1})

$$\Delta\mu_{O_2}\ (\pm 90) = (381 \pm 69) - (0.277 \pm 0.060)T. \quad (10)$$

Thus the precision achieved is slightly less than for the Cu + Cu_2O equilibrium, which may reflect the somewhat less reactive nature of the Fe + "FeO" electrode. The above equation has been used to amend the expressions for the Fe + "FeO" equilibrium to ($\mu_{O_2} \pm 100$ J·mol^{-1}; T in kelvins)

$$\begin{gathered} -605\,812 + 1366.718T - 182.7955T \ln T + 0.10359T^2 \\ (833 < T < 1042) \\ -519\,357 + 59.427T + 8.9276T \ln T \\ (1042 < T < 1184) \\ -551\,159 + 269.404T - 16.9484T \ln T. \\ (1184 < T < 1450) \end{gathered} \quad (11)$$

The agreement between the present results and the two-term expression given by Spencer and Kubaschewski (1978) is very good at temperatures above about 1200 K, but becomes increasingly less so at lower temperatures. This is mostly due to the inadequacy of a simple two-term expression, which implicitly neglects both the non-zero ΔC_P of the reaction and the phase transitions in Fe metal. A more detailed comparison with earlier studies is given in Holmes et al. (1986). It is noteworthy that the present results are in good agreement with the classic work of Darken and Gurry (1945), who used the CO-CO_2 gas-mixing method. Unfortunately, the same cannot be said for the recent work of Myers and Eugster (1983); their results are about 7000 J·mol^{-1} more oxidized at 1200 K.

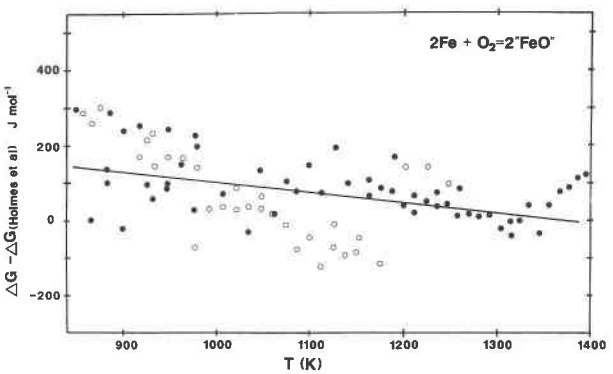

Fig. 4. Comparison of the present results for the reaction 2Fe + O_2 = 2"FeO" with those of Holmes et al. (1986). ●, data from runs starting with Fe + "FeO" (Table 2); ○, starting with Fe + Fe_3O_4 (Table 3).

Cu + Cu_2O vs. Fe + "FeO"—An experimental test

In order to test the results obtained for the Cu + Cu_2O and Fe + "FeO" equilibria measured against air, the following two types of cell were constructed:

$$\text{Pt, Fe + "FeO" | CSZ | Cu + } Cu_2O\text{, Pt} \quad \text{(IV)}$$
$$\text{Pt, Cu + } Cu_2O \text{ | CSZ | Fe + "FeO," Pt} \quad \text{(V)}$$

The difference between the two cells is purely geometrical. In the first, the Fe + "FeO" electrode occupied the sample position inside the CSZ tube with Cu + Cu_2O in the reference position, whereas in the second, these relative positions were reversed. Three runs were performed with the first type of cell and one with the second. Full experimental details are given in O'Neill (1987a), although the experiments with the first type of cell were actually done using an earlier design, which, although being similar to that shown in Figure 1 of O'Neill (1987a), differed in minor details. These cells were also not perfectly aligned relative to the "hot spot" of the furnace, necessitating small (<1 mV) corrections to compensate for the thermoelectric emf produced by the resulting temperature gradients, as described in O'Neill (1987a).

The results for the first type of cell are given in Table 4. The mean difference between these emf's and those that may be calculated from Equations 9 and 11 (i.e., from the measurements vs. air) is -0.27 ± 0.28 mV (note that 1 mV is equivalent to 386 J·mol^{-1}). Thus the agreement between the two methods is excellent and is almost within the combined precision of the air-reference experiments alone (± 100 J·mol^{-1}). The largest deviation of any of the 71 datum points is only 0.8 mV.

The results from the second type of cell (given in Table 5) are in even better agreement. The average deviation is $+0.06 \pm 0.11$ mV, which is close to the maximum precision that is possible to achieve with the method. These data are plotted against temperature in Figure 5, from

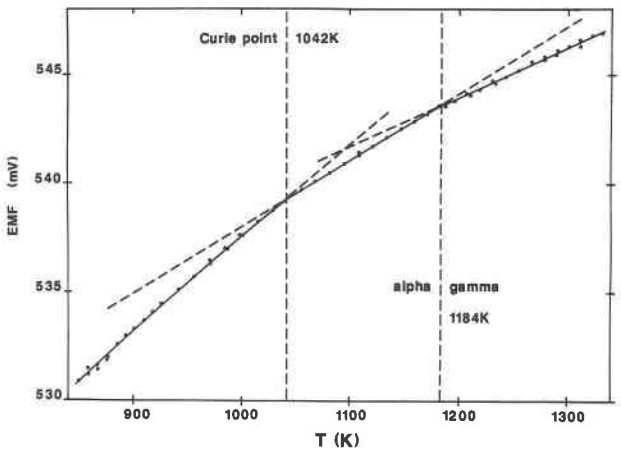

Fig. 5. Experimental results from the cell Pt, Cu + Cu_2O|CSZ|Fe + "FeO," Pt (Table 5). The lines (and their metastable extensions, shown dashed) are from Equations 9 and 11, obtained from the measurements vs. air. The breaks in slope caused by the Curie point and $\alpha \rightarrow \gamma$ transition in Fe are clearly discernible.

which it may be seen that the breaks in slope at the Curie point of Fe (1042 K) and $\alpha \rightarrow \gamma$ (1184 K) transitions are clearly distinguishable.

The excellent internal consistency shown by the two separate sets of experiments mean that the results on the Cu + Cu_2O and Fe + "FeO" equilibria may be used with some confidence.

Fe + Fe_3O_4

Results from cells with electrodes made from Fe and Fe_3O_4 are given in Table 3. The temperature range covered is from the lowest possible with the present experimental arrangement (750 K), up to the Fe + "FeO" + Fe_3O_4 isobaric invariant point at ~833 K.

Each datum has been analyzed to give the standard enthalpy at 298.15 K of the reaction

$$3Fe + 2O_2 = Fe_3O_4$$

using the third-law method:

$$\Delta_f H^0_{m,298.15} = \Delta_f G^0_{m,T} - \int_{298.15}^{T} \Delta_f C^0_{P,m} dT + T[\Delta_f S^0_{m,298.15} + \int_{298.15}^{T} (\Delta_f C^0_{P,m}/T)\, dT] \quad (13)$$

The calorimetric data used in this analysis are given in O'Neill (1987a). Those for Fe_3O_4 were taken from Robie et al. (1978), the choice of which is discussed in O'Neill (1987a). The calculated values of $\Delta_f H^0_{m,298.15}$ are plotted against the temperature of the datum in Figure 6.

The mean value of $\Delta_f H^0_{m,298.15}$ is -1115.39 ± 0.19 kJ·mol^{-1}, which is in exact agreement with that obtained, using the same calorimetric data, from a comparison of the Fe_2SiO_4 + Fe + SiO_2 (QFI) and Fe_2SiO_4 + Fe_3O_4 + SiO_2 (QFM) equilibria in O'Neill (1987a), in the range 1050 to 1320 K (-1115.43 ± 0.30 kJ·mol^{-1}). Note that the quoted errors do not include the uncertainties in the heat-capacity or entropy data. A mean value of -1115.4 kJ·mol^{-1} has been adopted. This value was then used with the same calorimetric data to calculate the free energy of formation of Fe_3O_4 at 20-K intervals from 760 to 1600 K. These values were regressed to give the following expressions for $\Delta_f G^0_{m,Fe_3O_4}$ (in J·mol^{-1}):

$$\begin{aligned}
&-1\,215\,345 + 2121.987T - 264.7817T \ln T \\
&+ 0.133\,140T^2 \quad (600 < T < 848) \\
&-1\,354\,650 + 4245.621T - 577.5478T \ln T \\
&+ 0.309\,515T^2 \quad (848 < T < 1042) \\
&-1\,079\,617 + 220.694T - 10.0979T \ln T \\
&\quad (1042 < T < 1184) \\
&-1\,116\,959 + 465.536T \\
&- 20.0438T \ln T. \quad (1184 < T < 1600)
\end{aligned} \quad (14)$$

TABLE 4. Results from the cells Pt, Fe + "FeO"|CSZ|Cu + Cu_2O, Pt

T (K)	emf (mV)	T (K)	emf (mV)	T (K)	emf (mV)
		Run 1			
1107	540.9	1021	537.8	1209	543.8
1037	538.5	1035	538.4	1222	544.2
977	536.2	1050	538.9	1234	544.5
946	535.5	1064	539.4	1247	544.7
945	535.2	1105	540.8	1260	544.8
912	533.6	1118	541.2	1272	545.2
878	532.6	1132	541.7	1284	545.5
896	532.5	1145	542.1	1295	545.7
913	533.3	1158	542.5	1307	546.0
929	534.0	1172	542.9	1318	546.2
991	536.6	1184	543.1	1328	546.5
1006	537.2	1196	543.4		
		Run 2			
855	530.8	936	535.3	1012	538.0
873	531.4	951	535.7	1012	537.9
889	532.3	967	536.3	1026	538.5
905	533.0	982	536.8	1040	539.2
921	533.9	998	537.7		
		Run 3			
914	533.0	1036	538.5	1170	542.9
946	534.5	1064	539.6	1194	543.5
978	536.3	1091	540.5	1220	544.6
1007	537.6	1119	541.5	1247	544.3
962	535.5	1078	540.1	1270	545.0
930	533.7	1105	540.8	1293	545.6
992	537.0	1131	541.6	1315	546.2
1021	537.9	1144	542.0		

"FeO" + Fe_3O_4

The "FeO" + Fe_3O_4 (wüstite-magnetite) equilibrium was studied using cells with M + MO mixtures as the reference electrodes, as were the other equilibria reported below. The advantages of this method have been discussed in O'Neill (1987a, 1987b), where full experimental details are given. In addition to Fe + "FeO" and Cu + Cu_2O, Ni + NiO was also used as a reference electrode; the calibration of μ_{O_2} for Ni + NiO has been reported in O'Neill (1987b) and is taken to be ($\mu_{O_2} \pm 120$ J·mol^{-1})

$$-480\,104 + 244.700T - 9.167T \ln T. \quad (800 < T < 1420) \quad (15)$$

The results for the cells

TABLE 5. Results from the cell Pt, Cu + Cu_2O|CSZ|Fe + "FeO," Pt

T (K)	emf (mV)	T (K)	emf (mV)	T (K)	emf (mV)
877	532.0	1042	539.2	1219	544.3
867	531.6	1056	539.7	1231	544.7
859	531.2	1069	540.1	1243	544.9
850	530.9	1082	540.5	1255	545.2
858	531.5	1096	540.9	1267	545.6
867	531.4	1109	541.3	1279	545.8
876	531.9	1082	540.5	1290	546.1
885	532.6	1056	539.7	1301	546.3
893	533.0	1029	538.7	1311	546.6
910	533.7	1000	537.6	1322	546.8
926	534.5	971	536.5	1300	546.3
942	535.1	1035	539.0	1279	545.7
957	535.7	1121	541.7	1211	544.0
971	536.3	1134	542.1	1188	543.5
986	537.0	1147	542.5	1234	544.6
901	533.3	1159	542.8	1267	545.6
917	534.1	1171	543.2	1289	545.9
987	537.0	1184	543.5	1311	546.3
1001	537.6	1109	541.4	1331	546.9
1015	538.2	1196	543.8		
1029	538.7	1207	544.1		

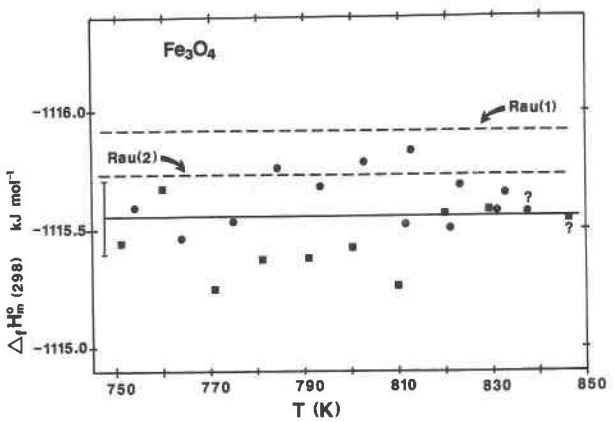

Fig. 6. The standard enthalpy of formation, $\Delta_f H^0_{m,298.15}$, of Fe_3O_4, calculated from the experimental data from the cells Pt, Fe + Fe_3O_4|CSZ|air, Pt, given in Table 3. ●, molar ratio of Fe to Fe_3O_4 is 4 to 1 (runs 1 and 2); ■, molar ratio of Fe to Fe_3O_4 is 1 to 2 (run 3). The two data annotated by question marks were obtained at temperatures above the Fe + "FeO" + Fe_3O_4 isobaric invariant point at ~833 K, where Fe + Fe_3O_4 is metastable. Also shown are the mean values obtained for this equilibrium by Rau (1972), using the reaction $3Fe + 4H_2O = Fe_3O_4 + 4H_2$, with a palladium H_2 membrane. The dashed line labeled Rau (1) refers to his data in the pure Fe-O system; that labeled Rau (2) refers to his data with Fe doped with 0.36 wt% Sn.

Pt, "FeO" + Fe_3O_4|CSZ|Fe + "FeO," Pt (VI)

Pt, "FeO" + Fe_3O_4|CSZ|Ni + NiO, Pt (VII)

are given in Table 6. Since the Fe + "FeO" equilibrium occurs at lower μ_{O_2}, and the Ni + NiO at higher, the "FeO" + Fe_3O_4 equilibrium is bracketed between the two, so that any errors resulting from the transfer of oxygen to or from the reference electrode will not bias the results.

It was found that the "FeO" + Fe_3O_4 electrodes appeared to react rapidly, with the emf of the cells coming quickly to the new equilibrium values on both raising and lowering temperature. However, the cells behaved in a very uncertain manner at higher temperatures (>1270 K), and the decrease in emf of the cell, which is eventually observed for all types of cell owing to the onset of oxygen transfer, was particularly marked. Hence no data are reported at temperatures higher than this. The emf's for the cell versus Ni + NiO below 920 K, while appearing quite steady, were obviously anomalous as they showed unusual fluctuations on changing temperature and were therefore also discarded.

The remaining data were regressed to give μ_{O_2} for "FeO" + Fe_3O_4 ($\mu_{O_2} \pm 306$ J·mol^{-1}):

$$-581\,927 - 65.618T + 38.7410T \ln T. \quad (833 < T < 1270) \quad (16)$$

The difference between each datum and the value given by this equation is illustrated in Figure 7. It may be seen that there is a significant difference between these residuals for each of the three runs, which is reflected in the rather larger than usual standard deviation of the equation. Since both types of cell have a fairly large temperature dependence of the cell emf, this could be explained by an error in the calibration of each thermocouple. (These runs were done over a period of some time and used thermocouples from different spools of wire, each needing a different calibration.) However, the problem was realized during the course of the latter two runs, and additional care was taken in calibrating the thermocouples after these runs. It is therefore felt that, at least in regard to these two runs, errors in temperature are not the cause of the difference.

The composition of "FeO" in equilibrium with Fe_3O_4 changes markedly with temperature, from $Fe_{0.945}O$ at the isobaric invariant point at 833 K to $Fe_{0.833}O$ at the "FeO" + Fe_3O_4 melting temperature at 1697 K (Spencer and Kubaschewski, 1978). This change in stoichiometry means that the extent of the reaction needed to reach equilibrium on changing temperature is far larger than for most equilibria involving phases with nearly constant stoichiometry, where the only equilibrium necessary is with the gas space above the electrode. The exceptions are those equilibria with a very high μ_{O_2}, where a substantial degree of reaction with the oxygen in the gas is required. An example is CoO + Co_3O_4, which was earlier studied in this laboratory (O'Neill, 1985) and which also showed a slightly larger than usual dispersion of the data, despite being apparently, like "FeO" + Fe_3O_4, very reactive.

Nevertheless, the uncertainty in the present results is still small compared to previous studies: ±306 J·mol^{-1} corresponds to only ±0.013 in $\log f_{O_2}$ at 1200 K. A comparison with some previous studies is given in Figure 8. Most of these are at somewhat higher temperatures, and extrapolation of the three-term equation for the present results must be uncertain owing not only to the large change in composition of "FeO," but also to the possi-

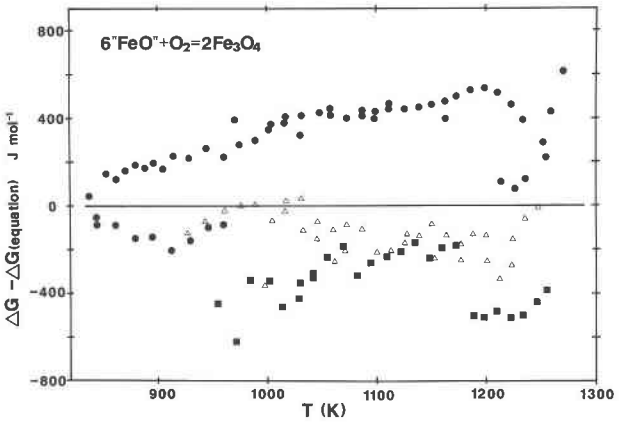

Fig. 7. Experimental results from the cells Pt, "FeO" + Fe_3O_4|CSZ|Fe + "FeO," Pt (■, run 1; ●, run 2, Table 6) and Pt, "FeO" + Fe_3O_4|CSZ|Ni + NiO, Pt (△, run 3), plotted as a function of temperature vs. the difference from Equation 16 in the text.

bility of one or more phase transitions in "FeO" at higher temperatures (e.g., Takayama and Kimizuka, 1980). A comparison with the calorimetric data has not been attempted because of these difficulties.

TABLE 6. Results from the cells Pt, "FeO" + Fe_3O_4|CSZ|Fe + "FeO," Pt and Pt, "FeO" + Fe_3O_4|CSZ|Ni + NiO, Pt

T (K)	emf (mV)	T (K)	emf (mV)	T (K)	emf (mV)	T (K)	emf (mV)
			Run 1 vs. (Fe + "FeO")				
1002	47.0	1015	50.4	1109	78.5	1198	104.3
1083	70.8	1029	54.6	1122	82.4	1210	107.9
1029	54.9	1042	58.8	1135	86.3	1222	111.6
1001	46.6	1056	62.8	1149	90.3	1234	115.3
986	42.4	1069	66.9	1160	93.9	1246	119.0
957	33.6	1082	70.8	1173	97.7	1257	122.6
971	37.3	1096	74.6	1186	100.7		
			Run 2 vs. (Fe + "FeO")				
961	35.8	897	18.1	1099	77.3	1186	103.4
945	31.3	905	20.5	1112	81.2	1198	107.1
930	26.6	913	22.9	1125	85.0	1210	110.6
913	21.8	929	27.4	1138	88.9	1162	96.0
897	17.3	945	32.0	1112	81.3	1221	114.1
880	12.5	960	36.4	1086	73.4	1234	117.5
863	7.8	975	40.8	1058	65.4	1257	124.1
845	2.9	990	45.2	1031	57.1	1270	129.0
838	1.1	1004	49.5	1003	49.1	1259	125.1
845	2.8	1018	53.7	973	40.5	1247	121.3
853	5.7	1032	57.8	1017	53.2	1236	117.5
862	8.1	1046	61.8	1098	76.9	1225	113.9
871	10.8	1059	65.8	1149	92.3	1213	110.5
880	13.4	1073	69.6	1162	96.0		
888	15.7	1086	73.5	1174	99.7		
			Run 3 vs. (Ni + NiO)				
928	223.6	1062	199.9	1176	177.7		
944	220.7	1031	204.9	1188	175.2		
961	217.6	1002	209.6	1200	172.8		
976	214.9	1017	207.6	1212	170.9		
990	212.4	1045	202.8	1224	168.3		
1005	209.9	1073	197.7	1201	172.9		
1018	207.3	1100	192.6	1177	177.7		
1033	204.9	1113	190.1	1152	182.6		
1046	202.4	1126	187.5	1127	187.2		
1060	199.9	1139	184.9	1224	168.0		
1073	197.4	1150	182.6	1236	165.3		
1086	195.0	1163	180.2	1248	162.7		

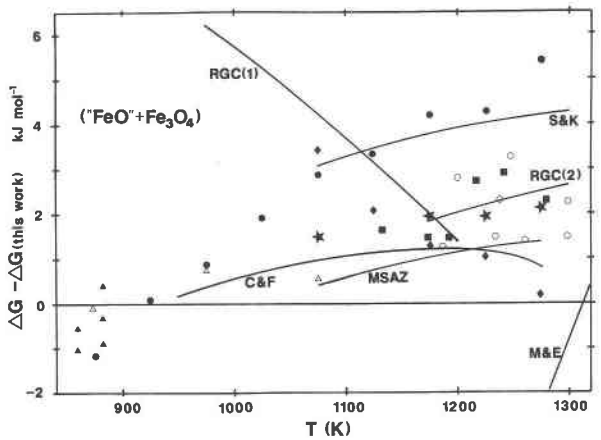

Fig. 8. Comparison of the present results for the "FeO" + Fe_3O_4 equilibrium with previous work at temperatures <1300 K. Equilibration with H_2-H_2O mixtures at 1 atm: △, Emmett and Shultz (1933); ▲, Rau (1972); ◆, Viktorovich et al. (1972). With CO-CO_2 mixtures and thermogravimetry: ■, Vallet and Raccah (1965). With CO_2-H_2 mixtures and thermogravimetry: M & E, Myers and Eugster (1983). Emf methods: ★, Roeder and Smeltzer (1964); ○, Levitskii et al. (1965); ●, Barbero et al. (1981); C & F, Charette and Flengas (1968); MSAZ, Moriyama et al. (1969); RGC, Rizzo et al. (1969) [(1) at 973–1202 K, (2) at 1173–1473 K]; S & K, Schwab and Küstner, 1981.

The Fe-"FeO"-Fe_3O_4 isobaric invariant point

The experimental results on the Fe + Fe_3O_4, Fe + "FeO," and "FeO" + Fe_3O_4 equilibria in the range 750 to 920 K are shown in Figure 9. The curves for these three equilibria should intersect at the isobaric invariant point where Fe + "FeO" + Fe_3O_4 coexist. The temperature of this point has been given by Spencer and Kubaschewski (1978) as 833 K, although there must be some uncertainty as to its exact location as it appears not to have been directly determined by reversed phase-equilibrium methods. Rau (1972) gave a temperature of 843 K, based on his H_2-H_2O equilibration measurements, and Emmett and Shultz (1933) gave 832 K. The intersection of the Fe + Fe_3O_4 and Fe + "FeO" curves given in the present work is at 826.8 K, and that of the "FeO" + Fe_3O_4 and Fe + "FeO" curves is at 833.9 K; there is thus excellent internal consistency in the present results, and excellent agreement with the phase diagram of Spencer and Kubaschewski (1978). It should be admitted that for the "FeO" + Fe_3O_4 equilibrium, the degree of agreement is rather better than the number of data at <900 K and the accuracy of the curve at higher temperatures would lead one to expect. It was intended to use the position of the isobaric invariant point to provide an additional constraint for the equation given for the "FeO" + Fe_3O_4 equilibrium, but this proved unnecessary.

The curves given for the Fe + "FeO" and "FeO" + Fe_3O_4 equilibria by Myers and Eugster (1983) intersect at 1052 K. The curve calculated for the Fe + Fe_3O_4 equilibrium from the QFI and QFM curves of Myers and

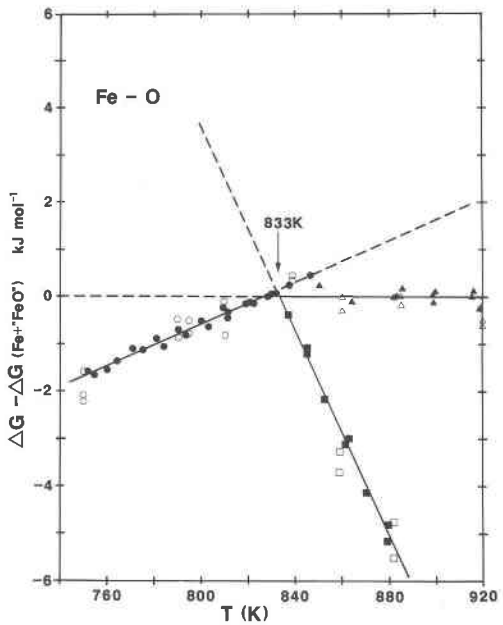

Fig. 9. Free energy for reactions: (1), Fe + Fe_3O_4, circles; (2), Fe + "FeO," triangles; and (3), "FeO" + Fe_3O_4, squares, plotted relative to Reaction 2, Fe + "FeO," in the range 750–920 K to show the position of the isobaric invariant point at which Fe + "FeO" + Fe_3O_4 coexist at 1 bar. Open symbols, Rau (1972); solid symbols, the present work.

Eugster intersects their Fe + "FeO" curve at −216 K (!) and their "FeO" + Fe_3O_4 curve at 1106 K, which gives some indication of the poor internal consistency of their results.

Fe_3O_4 + Fe_2O_3

The Fe_3O_4 + Fe_2O_3 equilibrium (magnetite-hematite, Reaction 4) is a very important one in petrology, not least because it is the basis of the Fe-Ti oxide geothermometer–oxygen barometer of Buddington and Lindsley (1964; and later versions). Two types of cell were used to study this equilibrium:

$$\text{Pt, } Fe_3O_4 + Fe_2O_3 \text{|CSZ|Cu + } Cu_2O\text{, Pt} \quad \text{(VIII)}$$
$$\text{Pt, } Fe_3O_4 + Fe_2O_3 \text{|CSZ|Ni + NiO, Pt} \quad \text{(IX)}$$

Two successful runs were done with cell VIII and one with cell IX. The results are given in Table 7. The μ_{O_2} of the Fe_3O_4 + Fe_2O_3 equilibrium intersects that of the Cu + Cu_2O equilibrium at ~1190 K. Below this temperature, Fe_3O_4 + Fe_2O_3 is stable at more reducing conditions than Cu + Cu_2O and is therefore bracketed between the latter and the Ni + NiO equilibrium. Above ~1190 K, Fe_3O_4 + Fe_2O_3 is more oxidizing than either of the reference electrodes, but is obviously closer to that of Cu + Cu_2O. Hence any errors introduced at high temperature due to oxygen transfer across the cell should be less for cell VIII than for cell IX.

Unlike all the other oxygen buffers used in this study, Fe_3O_4 + Fe_2O_3 proved to be extremely sluggish in its approach to equilibrium. In this regard it is similar to quartz-fayalite-magnetite (QFM) (O'Neill, 1987a). In all the runs attempted (which include some at temperatures below 1000 K, see below, that were not deemed successful and that are therefore not reported in detail), the initial emf was 50–100 mV more reduced than the inferred equilibrium value and decayed very slowly toward this value. This rate of decay decreased with decreasing temperature and was so slow that it would not be feasible to obtain measurements below about 1000 K, although the observed emf values at these lower temperatures eventually appeared constant and quite steady. These apparently stable emf values were, however, not reproducible from run to run (varying by up to 6 mV at any one temperature), were inconsistent with the calorimetric data when analyzed by the "third-law" method, and, on increasing temperature, gave rise to further long periods of slow decay.

The three successful runs were all begun at a temperature greater than 1000 K. A week was allowed in order to achieve equilibrium at the beginning of the run, by which time the emf had been observed to be constant to ±0.2 mV for at least 48 h. Thereafter, readings were taken ~48 h after increasing the temperature of the cell up to 1200 K, and thence at 24-h intervals. The time needed to achieve a stable emf on decreasing temperature was even longer; therefore, few such readings were attempted and then only toward the higher end of the temperature range covered by these experiments. Reversing the cells either by passing a small current across them or by flushing with a reducing or oxidizing gas was frustrated by the extremely long time needed to return to equilibrium; hence this procedure was not attempted in the runs reported in Table 7. Similarly sluggish behavior of Fe_3O_4 + Fe_2O_3

TABLE 7. Results from the cells Pt, Fe_3O_4 + Fe_2O_3|CSZ|Cu + Cu_2O, Pt and Pt, Fe_3O_4 + Fe_2O_3|CSZ|Ni + NiO, Pt

T (K)	emf (mV)	T (K)	emf (mV)	T (K)	emf (mV)	T (K)	emf (mV)
			Run 1 vs. (Cu + Cu_2O)				
1013	65.5	1121	24.5	1197	−6.0	1268	−35.5
1026	59.8	1134	19.7	1209	−10.8	1279	−39.9
1040	54.4	1146	14.7	1220	−15.3	1290	−44.4
1054	49.3	1158	10.0	1232	−19.9	1301	−48.5
1068	44.2	1171	5.2	1244	−25.4	1312	−53.0
1081	39.1	1183	−0.1	1256	−30.9	1322	−57.1
1094	33.9	1159	9.3	1245	−26.4	1301	−48.8
1107	29.2	1190	−3.4	1256	−31.0		
			Run 2 vs. (Cu + Cu_2O)				
1142	17.1	1205	−9.2	1264	−34.5	1320	−55.8
1155	12.3	1217	−14.5	1276	−39.0	1310	−51.7
1168	6.1	1229	−19.7	1287	−43.5	1299	−47.2
1180	0.8	1241	−24.8	1298	−47.7		
1193	−4.4	1253	−29.7	1309	−52.0		
			Run 3 vs. (Ni + NiO)				
1019	215.4	1101	240.6	1152	255.2	1224	279.3
1034	220.3	1074	231.5	1164	259.1	1235	283.1
1048	224.9	1100	239.8	1176	263.3	1247	286.5
1061	229.3	1114	243.8	1188	267.5	1258	290.3
1075	233.4	1127	247.6	1200	271.5	1268	293.6
1088	237.1	1140	251.4	1212	275.4		

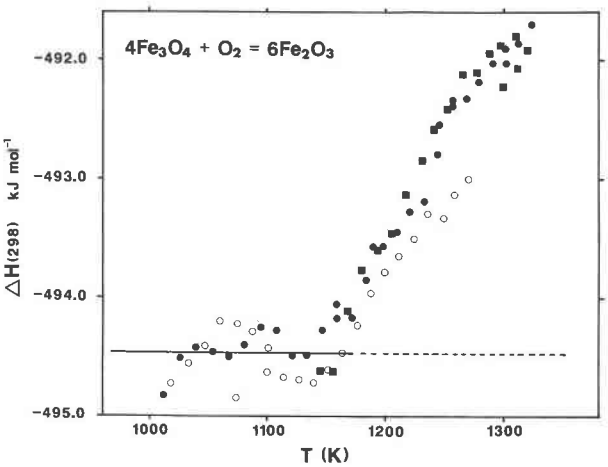

Fig. 10. Standard enthalpy, $\Delta_r H^0_{m,298.15}$, for the reaction $4Fe_3O_4 + O_2 = 6Fe_2O_3$ calculated from the experimental data in Table 7, using the entropy and heat-capacity data for Fe_3O_4, Fe_2O_3, and O_2 in Robie et al. (1978).

has been remarked on by Charette and Flengas (1968). It is emphasized, however, that all the data reported here are from measurements in which the emf values changed smoothly, if slowly, to the new value on changing temperature and thence remained perfectly constant (to within ±0.2 mV) until the next temperature increment.

Each datum was analyzed by the third-law method (Eq. 13) using the entropy and heat-capacity data for Fe_3O_4, Fe_2O_3, and O_2 given in Robie et al. (1978). The data for Fe_3O_4 have been previously shown to be consistent with the Fe + Fe_3O_4 (this work) and QFM (O'Neill, 1987a) emf measurements. The enthalpy of reaction at 298.15 K ($\Delta_r H^0_{m,298.15}$, Reaction 4) so obtained is plotted versus the temperature of the datum in Figure 10. Below ~1150 K, this enthalpy appears independent of temperature (within experimental error), and thus the emf measurements would seem to be in good agreement with the calorimetric data. However, the small temperature interval (~130 K) covered, coupled with the large coefficients of stoichiometry of the reaction (i.e., 6 mol of Fe_2O_3 and 4 mol of Fe_3O_4 per 1 mol of O_2) make this agreement less convincing than for the other equilibria studied in this work. The mean value of $\Delta_r H^0_{m,298.15}$ is -494.46 ± 0.2 kJ·mol^{-1}, which, with the previously deduced heat of formation of Fe_3O_4, gives $\Delta_f H^0_{m,298.15} = 826.0$ kJ·mol^{-1}. This compares satisfactorily with that measured by bomb calorimetry, 826.8 kJ·mol^{-1} (Roth, 1929).

Above 1173 K, the calculated $\Delta_r H^0_{m,298.15}$ values tend to be less negative. This is expected from the increasing solid solution of Fe_3O_4 toward γ-Fe_2O_3 above this temperature (e.g., Spencer and Kubaschewski, 1978). Dieckmann (1982) has measured the amount of nonstoichiometry in Fe_3O_4 (expressed as δ in $Fe_{3-\delta}O_4$) as a function of oxygen fugacity from 1173 to 1673 K. His data may be used to calculate the change in the activity of Fe_3O_4 in equilibrium with Fe_2O_3, relative to a standard state of stoichiometric Fe_3O_4, from the Gibbs-Duhem relation.

The formula $Fe_{3-\delta}O_4$ may be rewritten as $Fe_3O_4 + [2\delta/(3-\delta)]O_2$. The Gibbs-Duhem equation gives

$$RTd(\ln a_{Fe_3O_4}) = -(n_{O_2}/n_{Fe_3O_4})d\mu_{O_2} = [-2\delta/(3-\delta)]d\mu_{O_2}. \quad (17)$$

Dieckmann (1982) showed that δ is in fact a rather complicated function of μ_{O_2}, since besides the cation vacancies predominant at high μ_{O_2} values, Fe_3O_4 also possesses cation interstitials, which dominate at low μ_{O_2}. The overall value of δ is therefore a product of two independent defect equilibria. However, at the high μ_{O_2} values of interest here, cation vacancies greatly outnumber interstitials; hence, to a good approximation, the latter may be ignored. Dieckmann found that δ in this region depends on f_{O_2} according to the relation

$$\delta \propto (f_{O_2})^{1/5} \quad (18)$$

and hence

$$d\mu_{O_2} = -(3RT/2\delta)\, d\delta. \quad (19)$$

Substituting this into Equation 17 and integrating from $\delta = 0$ to δ gives

$$RT \ln a_{Fe_3O_4} = 3RT \ln(3-\delta)/3.$$

The values of δ at the μ_{O_2} of the $Fe_3O_4 + Fe_2O_3$ equilibrium were then calculated from Equation 13 in Dieckmann (1982), at 1173, 1273, and 1373 K, to give the following values of $RT \ln a_{Fe_3O_4}$ at these temperatures (in J·mol^{-1}): 66, 165, and 318. Since there are 4 mol of Fe_3O_4 per 1 mol of O_2 for the $Fe_3O_4 + Fe_2O_3$ equilibrium, the expected deviation from a horizontal line for $\Delta_r H^0_{m,298.15}$ in Figure 10 would then be 0.26 kJ at 1173 K, 0.66 kJ at 1273 K, and 1.27 kJ at 1373 K. This deviation is only about half that observed, which may indicate that the calorimetric data for Fe_2O_3 are in fact slightly in error, with the small temperature range covered by the emf measurements reported here at temperatures less than 1150 K being insufficient for such errors to be noticeable. Note that since there are 6 mol of Fe_2O_3 per 1 mol of O_2 in the $Fe_3O_4 + Fe_2O_3$ equilibrium, quite small errors in the entropy for Fe_2O_3 may be multiplied to produce a fairly substantial effect on the calculated $\Delta_r H^0_{m,298.15}$

The results of some previous work on the $Fe_3O_4 + Fe_2O_3$ oxygen buffer are summarized in Figure 11. The emf study of Blumenthal and Whitmore (1961) is in excellent agreement with the present results, and that of Moriyama et al. (1969) in good agreement. However, most of the previous emf studies, including some in which the experimental design has been shown to perform satisfactorily in the determination of other, less kinetically sluggish equilibria, are tightly clustered in a region ~6 kJ·mol^{-1} more oxidized than these results. It is worth noting, though, that none of these studies show the change in slope of $\Delta_r H^0_{m,298.15}$ expected from the increasing departure from stoichiometry of Fe_3O_4 above ~1150 K. The results

of Rau (1972) at lower temperatures—which were obtained using the same H_2-H_2O method as for the Fe + Fe_3O_4, Fe + "FeO," and "FeO" + Fe_3O_4 equilibria and which were in excellent agreement with the emf measurements reported earlier in this paper—are even more oxidized, by ~10 kJ·mol^{-1}. However, it might be expected that, in this case, Rau's method would not be particularly accurate, as the partial pressure of H_2 in H_2-H_2O mixtures in equilibrium with Fe_3O_4 + Fe_2O_3 at atmospheric pressure is very low and consequently difficult to measure with the necessary precision. It is also worth noting that the material used by Rau was very fine grained iron hydroxides dehydrated at 300 °C and may well be in a state metastable to true, well-crystallized α-Fe_2O_3. The H_2-sensor method of Chou (1978) is the only hydrothermal study of this equilibrium that I have found in the literature. Chou's results are in good agreement with the present ones above 973 K, but tend toward more negative values of $\Delta_r H^0_{m,298.15}$ at lower temperatures. Interestingly, this trend is similar to that shown by my attempted measurements at T < 1000 K, which were interpreted not to have fully reached equilibrium (and which are thus not reported in detail); these actually gave, for example, $\Delta_r H^0_{m,298.15}$ between −497.5 and −499.5 kJ·mol^{-1} at ~820 K.

The discrepancy between this majority of previous emf studies and this work is too large to be explained by the usual experimental uncertainties of the emf method, which mostly amount to <2 kJ·mol^{-1} [see, for example, the comparisons illustrated in Fig. 6 of Holmes et al. (1986) for the Cu + Cu_2O, Ni + NiO, Co + CoO, and Fe + "FeO" buffers]. That the present results are "more reduced" is especially disconcerting when it is remembered that in all runs the emf's approached stable values slowly from the reducing side. It is therefore possible that the present results represent a metastable equilibrium; if so, it is a highly persistent one, as, for example, the runs reported in Table 7 typically were held at temperatures greater than ~1020 K for periods in excess of two months. Furthermore, the hydrothermal work of Chou should be less liable to such metastability because H_2O at high pressures may promote equilibrium through dissolution and reprecipitation processes and, as pointed out above, Chou's results are in reasonably good agreement. Conversely, if the present results are indeed accurate, then the majority of the previous emf work might equally well be recording a metastable equilibrium—perhaps involving γ-Fe_2O_3. This is plausible since γ-Fe_2O_3 is less stable than α-Fe_2O_3; therefore, the Fe_3O_4 + γ-Fe_2O_3 metastable equilibrium must occur at higher μ_{O_2} than the stable Fe_3O_4 + α-Fe_2O_3 equilibrium. XRD analysis of the sample pellets after each of the runs in Table 7 showed only the expected pattern of well-crystallized Fe_3O_4 and α-Fe_2O_3. Also, the solubility of Fe in Pt metal at the μ_{O_2} of the Fe_3O_4 + Fe_2O_3 equilibrium at the temperatures of this study is negligible, and there was no evidence for any other side reaction in the cell.

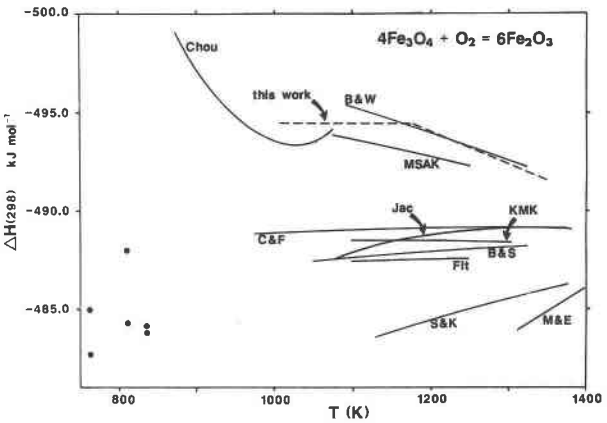

Fig. 11. Comparison of the present results for the Fe_3O_4 + Fe_2O_3 equilibrium with earlier work at temperatures <1350 K. ●, Rau (1972), H_2-H_2O equilibrium at 1 bar; C, Chou (1978), H_2-sensor at 2 and 4 kbar; M & E, Myers and Eugster (1983), CO_2-H_2 and thermogravimetry. The others all used an emf method: B & W, Blumenthal and Whitmore (1961); C & F, Charette and Flengas (1968); MSAZ, Moriyama et al. (1969); B & S, Bryant and Smeltzer (1969); F, Fitzner (1979); KMK, Katayama et al. (1980); S & K, Schwab and Küstner (1981); J, Jacobsson (1985).

Finally, the inconsistency between the different emf experiments on the Fe_3O_4 + Fe_2O_3 equilibrium seems to extend to similar experiments that seek to use this equilibrium to determine the activity of Fe_3O_4 in spinel solid solutions. Thus activity-composition relations in $ZnFe_2O_4$-Fe_3O_4 solutions in equilibrium with Fe_2O_3 have now been measured no less than four times. Two studies (Katayama et al., 1977; Schaefer and McCune, 1986) report very small positive deviations from ideality, but two others (Tretyakov, 1967; Fitzner, 1979) report substantial negative deviations, the difference between the two schools amounting to ~30 mV in the cell emf for the composition $X_{Fe_3O_4} = 0.5$ at 1173 K, which is about twice that between the present results and the majority for the univariant equilibria. Earlier work with a gas-equilibration method (Benner and Kenworthy, 1966) sheds no light on the problem, as these authors obtained a third kind of result, large positive deviations from ideality.

Cu_2O + CuO

The experimental results from the cell

$$\text{Pt, } Cu_2O + CuO|CSZ|Cu + Cu_2O, \text{ Pt} \qquad \text{(X)}$$

are given in Table 8. No problems were encountered with this cell, and stable emf values were achieved rapidly at all temperatures. The data were analyzed in the same way as those for the Cu + Cu_2O equilibrium. Values of μ_{O_2} for the reaction

$$2Cu_2O + O_2 = 4CuO \qquad (20)$$

were taken from the JANAF tables (Chase et al., 1982)

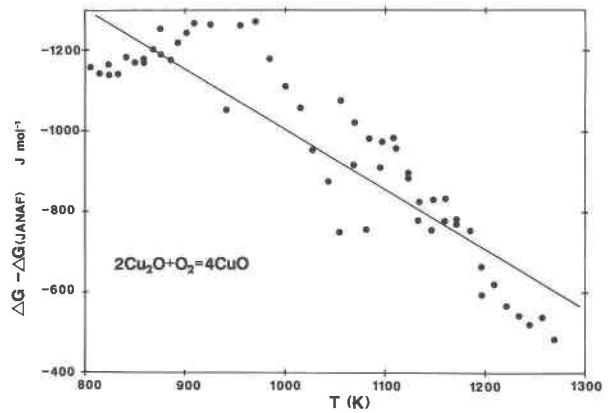

Fig. 12. Comparison of the results for the free energy of the reaction $2Cu_2O + O_2 = 4CuO$ with those derived from calorimetric data as assessed in the JANAF tables (Chase et al., 1982).

for Cu_2O and CuO from 700 to 1300 K inclusive and, after correcting from the reference pressure of 1 atm to 1 bar, were fitted by least squares to give the expression

$$\mu_{O_2}^{(Cu_2O+CuO)}{}_{JANAF} = -289\,748 + 375.522T - 23.1976T \ln T. \quad (21)$$

For each datum, the difference $\Delta\mu_{O_2} = \mu_{O_2,obs} - \mu_{O_2,JANAF}$ was calculated and has been plotted against the temperature of the measurement in Figure 12. Regression of $\Delta\mu_{O_2}$ versus T gives

$$\Delta\mu_{O_2}\ (\pm 99) = (2497 \pm 99) + (1.490 \pm 0.095)T. \quad (22)$$

Since the uncertainties quoted in the JANAF tables for $\Delta_f H^0_{m,298.15}$ and $S^0_{m,298.15}$ for CuO are ± 2.09 kJ·mol^{-1} and ± 0.42 J·K^{-1}·mol^{-1}, respectively, the deviation of the present results from the calorimetric data, as shown by Equation 22, is within the uncertainty limits of the latter. The expression for the chemical potential of oxygen defined by the Cu_2O + CuO equilibrium may therefore be amended to ($\mu_{O_2} \pm 117$ J·mol^{-1}; T in kelvins)

$$-292\,245 + 377.012T - 23.1976T \ln T. \quad (800 < T < 1300)$$

The results of Charette and Flengas (1968), which were obtained in a cell with Ni + NiO as the reference electrode in the temperature range 892 to 1320 K, differ from the above by approximately +1.4 kJ·mol^{-1}. The more recent work of Peters (1983), who used an emf cell with air as the reference, differs by amounts varying from +1.7 kJ·mol^{-1} at 973 K to −6.3 kJ·mol^{-1} at 1323 K and is thus evidently at odds with the calorimetric data.

The Cu_2O + CuO equilibrium could prove useful as an oxygen buffer in hydrothermal experiments where a high f_{O_2} (or low f_{H_2}) is required.

Conclusions

The μ_{O_2} defined by the Cu + Cu_2O and Fe + "FeO" equilibria have been determined to a very high degree of absolute accuracy using an electrochemical method with air as the reference electrode. The results are in good agreement with the earlier work from this laboratory by Holmes et al. (1986) and are indeed within the stated error limits of the latter, but represent an improvement in both precision and accuracy that is due to minor modifications in the experimental technique. These are principally (a) the use of *two* accurately calibrated thermocouples, to eliminate any problems with small temperature gradients; (b) the use of YDT versus air electrodes, which enables data to be obtained at temperatures as low as 750 K (vs. 900 K for Holmes et al.); and (c) increasing the accuracy with which the μ_{O_2} of air is measured, by taking into account the partial pressure of water vapor in the atmosphere, which is somewhat variable.

TABLE 8. Results for the cell Pt, Cu_2O + CuO|CSZ|Cu + Cu_2O, Pt

T (K)	emf (mV)	T (K)	emf (mV)	T (K)	emf (mV)	T (K)	emf (mV)
876	282.4	892	284.6	1081	309.4	1083	309.0
859	280.4	901	285.6	1094	310.6	1055	305.4
841	278.1	909	286.6	1107	312.0	1069	307.2
823	275.8	925	288.6	1121	313.9	1096	310.6
804	273.3	939	291.0	1134	315.7	1122	314.0
813	274.6	955	292.4	1146	317.3	1196	323.7
823	275.9	970	294.3	1158	318.7	1208	325.1
832	277.1	984	296.3	1171	320.2	1221	326.7
841	278.1	999	298.3	1184	321.8	1233	328.2
850	279.3	1013	300.2	1172	320.3	1209	325.1
859	280.5	1027	302.2	1160	318.7	1245	329.4
868	281.5	1041	304.2	1148	317.3	1257	331.1
876	282.6	1055	306.2	1135	315.8	1269	332.6
884	283.7	1068	307.3	1110	312.3		

For Cu + Cu_2O, the results are in essentially perfect agreement with the very precise calorimetric data of Mah et al. (1967) and Chase et al. (1982). In other words, these results provide an excellent experimental proof of the third law of thermodynamics. For Fe + "FeO," agreement with the calorimetric data is also good, as is the agreement with the values recommended by Spencer and Kubaschewski (1978) from an appraisal of 35 previous studies.

The results of these experiments with air as the reference electrode have in addition been checked by measuring Cu + Cu_2O directly against Fe + "FeO" and vice versa. They may therefore be adopted with confidence.

The Fe + Fe_3O_4 equilibrium was also studied using air as the reference. The accessible temperature range for this equilibrium is restricted to temperatures below 833 K, above which Fe reacts with Fe_3O_4 to form "FeO." Nevertheless, the results obtained in this narrow temperature region are fully consistent with those deduced earlier (O'Neill, 1987a) from a comparison of the Fe + Fe_2SiO_4 + SiO_2 and Fe_3O_4 + Fe_2SiO_4 + SiO_2 equilibria at higher temperatures (1050–1320 K).

The "FeO" + Fe_3O_4 equilibrium was studied using Fe + "FeO" and Ni + NiO as reference electrodes. This equilibrium was found to intersect the Fe + "FeO" and Fe + Fe_3O_4 equilibria at the isobaric invariant point of 833 K, which therefore demonstrates good internal consisten-

cy. Agreement with the results of Rau (1972), who used a H_2-H_2O equilibration method, are excellent.

The results for $Fe_3O_4 + Fe_2O_3$ are less satisfactory. The exceptionally sluggish approach to equilibrium shown by this assemblage makes demonstration of equilibrium by reversal difficult and also limits the temperature range of investigation that is practical with the present method to above about 1000 K. Although the agreement of the results with existing calorimetric data appears quite good, this test is rendered somewhat uncertain by the large coefficients of stoichiometry of the reaction (i.e., 6 mol of Fe_2O_3 and 4 mol of Fe_3O_4 to 1 mol of O_2), by the Curie points of Fe_3O_4 at 850 K and Fe_2O_3 at 950 K, and by the increasingly large degree of nonstoichiometry in Fe_3O_4 above about 1150 K. Comparison with previous studies reveals that most of these place the equilibrium at a position more oxidizing by some 6 $kJ \cdot mol^{-1}$ in μ_{O_2}. This may be due to metastability of the crystalline form of Fe_2O_3, but, in order to ascertain this, further experiments with a technique that increases the rate of equilibration (e.g., by using a flux) would be necessary at lower temperatures.

Acknowledgments

I would like to thank Professor A. E. Ringwood for providing laboratory facilities, Herb Niessler for help with the electronics, Paul Willis and Bill Hibberson for technical assistance, and Stefan Seifert for taking some of the readings during my absences from the laboratory. The Canberra Bureau of Meteorology kindly loaned a psychrometer. This work grew out of the earlier collaboration with Dick Arculus and Richard Holmes, whose insights into the techniques of solid electrolyte measurements are gratefully acknowledged. Sue Kesson is thanked for reading and correcting an earlier version of this paper and Dick Arculus and Ricardo Aragon for helpful reviews.

References cited

Alcock, C.B., Fitzner, K., and Jacob, K.T. (1977) An entropy meter based on the thermo-electric potential of a nonisothermal solid-electrolyte cell. Journal of Chemical Thermodynamics, 9, 1011–1020.

Badwal, S.P.S. (1983) New electrode materials for low temperature oxygen sensors. Journal of Electroanalytical Chemistry, 146, 425–429.

——— (1984) Kinetics of the oxygen transfer reaction at the $(U_{0.5}Sc_{0.5})O_{2\pm x}$–YSZ interface by impedance spectroscopy. Journal of Electroanalytical Chemistry, 161, 75–91.

Bannister, M.J. (1984) The standard molar Gibbs free energy of formation of PbO. Oxygen concentration-cell measurements. Journal of Chemical Thermodynamics, 16, 787–792.

Barbero, J.A., Blesa, M.A., and Maroto, A.J.G. (1981) The lower temperature range of the wüstite stability field. Zeitschrift für Physikalische Chemie Neue Folge, 124, 139–147.

Benner, R.L., and Kenworthy, H. (1966) The thermodynamic properties of the ZnO-Fe_2O_3-Fe_3O_4 system at elevated temperatures. U.S. Bureau of Mines Report of Investigation 6769.

Berglund, S. (1976) The free energy of formation of nickel oxide. Berichte der Bunsen-Gesellschaft für Physikalische Chemie, 80, 862–866.

Blumenthal, R.N., and Whitmore, D.H. (1961) Electrochemical measurements of elevated-temperature thermodynamic properties of certain iron and manganese oxide mixtures. Journal of the American Ceramic Society, 44, 508–512.

Bryant, P.E.C., and Smeltzer, W.W. (1969) The dissociation pressure of hematite. Journal of the Electrochemical Society, 116, 1409–1410.

Buddington, A.F., and Lindsley, D.H. (1964) Iron-titanium oxide minerals and synthetic equivalents. Journal of Petrology, 5, 310–357.

Charette, G.G., and Flengas, S.N. (1968) Thermodynamic properties of the oxides of Fe, Ni, Pb, Cu and Mn, by EMF measurements. Journal of the Electrochemical Society, 115, 796–804.

Chase, M.W., Jr., Curnutt, J.L., Downey, J.R., McDonald, R.A., Syverud, A.N., and Valenzuela, E.A. (1982) JANAF thermochemical tables, 1982 supplement. Journal of Physical and Chemical Reference Data, 11, 695–940.

Chou, I-M. (1978) Calibration of oxygen buffers at elevated P and T using the hydrogen fugacity sensor. American Mineralogist, 63, 690–703.

Choudhary, C.B., Maiti, H.S., and Subbarao, E.C. (1980) Defect structures and transport properties. In E.C. Subbarao, Ed., Solid electrolytes and their applications, p. 1–80. Plenum Press, New York.

Comert, H., and Pratt, J.N. (1982) The thermodynamic properties of solid cobalt-zinc alloys. Thermochimica Acta, 59, 267–285.

Darken, L.S., and Gurry, R.W. (1945) The system iron-oxygen. I. The wüstite field and related equilibria. Journal of the American Chemical Society, 67, 1398–1412.

Dieckmann, R. (1982) Defects and cation diffusion in magnetite (IV): Nonstoichiometry and point defect structure of magnetite ($Fe_{3-\delta}O_4$). Berichte der Bunsen-Gesellschaft für Physikalische Chemie, 86, 112–118.

Emmett, P.H., and Shultz, J.F. (1933) Gaseous thermal diffusion—The principal cause of discrepancies among equilibrium measurements on the systems Fe_3O_4-H_2-Fe-H_2O, Fe_3O_4-H_2-FeO-H_2O and FeO-H_2-Fe-H_2O. Journal of the American Chemical Society, 55, 1376–1389.

Fitzner, K. (1979) Thermodynamic properties and cation distribution of the $ZnFe_2O_4$-Fe_3O_4 spinel solid solution at 900°C. Thermochimica Acta, 31, 227–236.

Holmes, R.D., O'Neill, H.St.C., and Arculus, R.J. (1986) Standard Gibbs free energy of formation for Cu_2O, NiO, CoO and Fe_xO: High-resolution electrochemical measurements using zirconia solid electrolytes from 900–1400 K. Geochimica et Cosmochimica Acta, 50, 2439–2452.

Jacobsson, E. (1985) Solid state EMF studies of the systems FeO-Fe_3O_4 and Fe_3O_4-Fe_2O_3 in the temperature range 1000–1600 K. Scandinavian Journal of Metallurgy, 14, 252–256.

Jacobsson, E., and Rosén, E. (1981) Thermodynamic studies of high temperature equilibria. 25. Solid state EMF studies of the systems Fe-FeO, Ni-NiO and Co-CoO in the temperature range 1000–1600 K. Scandinavian Journal of Metallurgy, 10, 39–43.

Katayama, I., Shibata, J., Aoki, M., and Kozuka, Z. (1977) Thermodynamic study of spinel type solid solutions of the Fe_3O_4-$ZnFe_2O_4$ system by E.M.F. measurements using the solid electrolyte. Transactions of the Japanese Institute of Metals, 18, 744–749.

Katayama, I., Matsuda, T., and Kozuka, Z. (1980) Thermodynamic study on Fe_3O_4-$CuFe_2O_4$ system by E.M.F. method. Technology Reports of the Osaka University, 30, 385–390.

Kermori, N., Katayama, I., and Kozuka, Z. (1979) Measurement of standard molar Gibbs energies of formation of NiO, Cu_2O, and CoO from solid and liquid metals and oxygen gas by an emf method at high temperatures. Journal of Chemical Thermodynamics, 11, 215–228.

Levitskii, V.A., Rezukhina, T.N., and Dneprova, V.G. (1965) Measurement of the EMF from galvanic cells with a solid electrolyte above 1100°C. Soviet Electrochemistry, 1, 833–839.

Mah, A.D., Pankratz, L.B., Weller, W.W., and King, E.G. (1967) Thermodynamic data for cuprous and cupric oxides. U.S. Bureau of Mines Report of Investigation 7026.

Moriyama, J., Sato, N., Asao, H., and Kozuka, Z. (1969) Thermodynamic study on the systems of metals and their oxides by EMF measurements using solid electrolyte. Memoirs of the Faculty of Engineering, Kyoto University, 31, 253–267.

Myers, J., and Eugster, H.P. (1983) The system Fe-Si-O: Oxygen buffer calibrations to 1,500 K. Contributions to Mineralogy and Petrology, 82, 75–90.

O'Neill, H.St.C. (1985) Thermodynamics of Co_3O_4: A possible electron spin unpairing transition in Co^{3+}. Physics and Chemistry of Minerals, 12, 149–154.

——— (1987a) Quartz-fayalite-iron and quartz-fayalite-magnetite equilibria and the free energy of formation of fayalite (Fe_2SiO_4) and magnetite (Fe_3O_4). American Mineralogist, 72, 67–75.

——— (1987b) Free energies of formation of NiO, CoO, Ni_2SiO_4, and Co_2SiO_4. American Mineralogist, 72, 280–291.

Peters, T. (1983) Equilibrium fugacities of the Cu_2O-CuO and Cu-Cu_2O

buffers. Schweizerische Mineralogische und Petrologische Mitteilungen, 63, 7–11.

Rau, H. (1972) Thermodynamics of the reduction of iron oxide powders with hydrogen. Journal of Chemical Thermodynamics, 4, 57–64.

Rizzo, F.E., Gordon, R.S., and Cutler, I.B. (1969) The determination of phase boundaries and thermodynamic functions in the iron-oxygen system by EMF measurements. Journal of the Electrochemical Society, 116, 266–274.

Robie, R.A., Hemingway, B.S., and Fisher, J.R. (1978) Thermodynamic properties of minerals and related substances at 298.15 K and 1 bar (10^5 pascals) and at higher temperatures. U.S. Geological Survey Bulletin 1452.

Roeder, G.A., and Smeltzer, W.W. (1964) The dissociation pressures of iron-nickel oxides. Journal of the Electrochemical Society, 111, 1074–1078.

Rossini, F.D. (1970) Report on the International Practical Temperature Scale of 1968. Journal of Chemical Thermodynamics, 2, 447–459.

Roth, W.A. (1929) Beiträge zur Thermochemie des Eisens, Mangans und Nickels. Archiv für das Eisenhüttenwesen, 3, 339–346.

Santander, N.H., and Kubaschewski, O. (1975) The thermodynamics of the copper-oxygen system. High Temperatures–High Pressures, 7, 573–582.

Schaefer, S.C., and McCune, R.A. (1986) Electrochemical determination of thermodynamic properties and X-ray diffraction investigation of the Fe_3O_4-$ZnFe_2O_4$ system. Metallurgical Transactions, 17B, 515–521.

Schwab, R.G., and Küstner, D. (1981) Die Gleichgewichtsfugazitäten technologisch und petrologisch wichtiger Sauerstoffpuffer. Neues Jahrbuch für Mineralogie Abhandlungen, 140, 111–142.

Spencer, P.J., and Kubaschewski, O. (1978) A thermodynamic assessment of the iron-oxygen system. CALPHAD, 2, 147–167.

Stull, D.R., and Prophet, H. (1971) JANAF thermochemical tables (2nd edition). U.S. National Bureau of Standards, National Standard Reference Data Series 37, 1141 p.

Takayama, E., and Kimizuka, N. (1980) Thermodynamic properties and subphases of wüstite field determined by means of thermogravimetric method in the temperature range of 1100–1300°C. Journal of the Electrochemical Society, 127, 970–975.

Tretyakov, Y.D. (1967) "Thermodynamika Ferritov." Izdatel Khimiya Leningradskoe Otdel. Leningrad, USSR.

Vallet, P., and Raccah, P. (1965) Contribution à l'étude des propriétés thermodynamiques du protoxyde de fer solide. Mémoires Scientifiques et Revue de Metallurgie, 62, 1–29.

Viktorovich, G.S., Lisovskii, D.I., and Zhaglov, V.S. (1972) Thermodynamics of the equilibrium between wüstite and metallic iron or magnetite and the hydrogen-water gas phase. Russian Journal of Physical Chemistry, 46, 882.

Worrell, W.L., and Iskoe, J.L. (1973) Kinetics of oxygen transfer at the interface between a zirconia-based electrolyte and a metal–metal oxide electrode. In W. van Gool, Ed., Fast ion transport in solids, p. 513–521. North-Holland, Amsterdam.

Manuscript received May 7, 1987
Manuscript accepted January 8, 1988